



Published in final edited form as:

*Circ Res.* 2023 August 18; 133(5): 412–429. doi:10.1161/CIRCRESAHA.123.323030.

## T-Cell MyD88 Is a Novel Regulator of Cardiac Fibrosis Through Modulation of T-Cell Activation

Abraham L. Bayer, B.S.<sup>1</sup>, Sasha Smolgovsky, M.S.<sup>1</sup>, Njabulo Ngwenyama, PhD<sup>1</sup>, Ana Hernández-Martínez, B.S.<sup>1</sup>, Kuljeet Kaur, PhD<sup>1</sup>, Katherine Sulka, B.S.<sup>1</sup>, Junedh Amrute, B.S.<sup>2</sup>, Mark Aronovitz, M.S.<sup>1</sup>, Kory Lavine, M.D. PhD<sup>2</sup>, Shruti Sharma, PhD<sup>1</sup>, Pilar Alcaide, PhD<sup>1</sup>

<sup>1</sup>Department of Immunology, Tufts University, Boston MA

<sup>2</sup>Department of Medicine, Washington University School of Medicine, Saint Louis MO

### Abstract

**Background:** Cardiac inflammation in heart failure (HF) is characterized by the presence of damage associated molecular patterns (DAMPs), myeloid cells, and T-cells. Cardiac DAMPs provide continuous pro-inflammatory signals to myeloid cells through toll-like receptors (TLRs) that converge onto the adaptor protein “Myeloid Differentiation Response 88” (MyD88). These induce activation into efficient antigen presenting cells that activate T-cells through their T-cell receptor (TCR). T-cell activation results in cardiotropism, cardiac fibroblast (CFB) transformation, and maladaptive cardiac remodeling. T-cells rely on TCR signaling for effector function and survival, and while they express MyD88 and DAMP receptors, their role in T-cell activation and cardiac inflammation is unknown.

**Methods:** We performed transverse aortic constriction (TAC) in mice lacking MyD88 in T-cells and analyzed remodeling, systolic function, survival, and T-cell activation. We profiled WT vs. *Myd88*<sup>-/-</sup> mouse T-cells at the transcript and protein level and performed several functional assays.

**Results:** Analysis of single cell RNA-seq data sets revealed that MyD88 is expressed in mouse and human cardiac T-cells. MyD88 deletion in T-cells resulted in increased levels of cardiac T-cell infiltration and fibrosis in response to TAC. We discovered that TCR-activated *Myd88*<sup>-/-</sup> T-cells had increased pro-inflammatory signaling at the transcript and protein level compared to WT, resulting in increased T-cell effector functions such as adhesion, migration across endothelial cells,

---

**Corresponding Author:** Pilar Alcaide, pilar.alcaide@tufts.edu, 137 Harrison Ave, Boston MA, 02111.

#### Author Contributions

A.L.B designed the project, performed experiments, analyzed data, and wrote the manuscript. S.S. and K.K. performed experiments and edited the manuscript. N.N. and A.H. designed and performed experiments. M.A. performed all TAC surgeries. K.L. and J.A. generated and analyzed the human single cell data, and K.S. and S.S. analyzed the mouse single cell data. P.A. designed the project, provided intellectual support, and edited the manuscript.

#### Conflicts of Interest:

The authors declare no conflicts of interest.

#### Supplemental Materials:

Supplemental Methods

Tables S1–S2

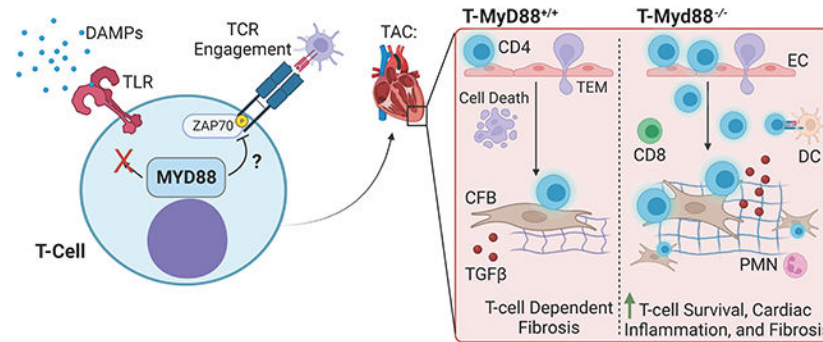
Figures S1–S11

Major Resources Table

and activation of CFB. Mechanistically, we found that MyD88 modulates T-cell activation and survival through TCR-dependent, rather than TLR dependent signaling.

**Conclusion:** Our results outline a novel intrinsic role for MyD88 in limiting T-cell activation that is central to tune down cardiac inflammation during cardiac adaptation to stress.

### Graphical Abstract



### Subject Terms:

Fibrosis; Pathology

### Keywords

Heart Failure; Inflammation; T-cells; MyD88; DAMPs

### Introduction:

Cardiac inflammation and cardiac fibrosis are two intimately associated hallmarks of HF, however thus far anti-inflammatory therapies have shown limited success in clinical trials.<sup>1-3</sup> This suggests a more in depth study of specific inflammatory mechanisms is needed to improve anti-inflammatory therapies in HF. As cardiac damage ensues, the constant release of damage associated molecular patterns (DAMPs) activates resident myeloid cells to present antigen to T-cells in a continuous progression of worsening inflammation.<sup>4,5</sup> DAMPs, also known as “alarmins,” are increased in the heart during HF.<sup>6,7</sup> Most DAMP receptors, such as toll-like receptors (TLRs) and the IL-1 family of receptors, converge onto the adaptor protein Myeloid differentiation primary response protein 88 (MyD88), to initiate an innate immune response.<sup>8,9</sup> The persistent inflammation initiated through DAMP-myeloid-MyD88 signaling during HF suggests that intrinsic mechanisms must exist to resolve or mitigate a continuous subsequent T-cell immune response during cardiac maladaptive adaptations to stress.

We previously showed that antigen presentation by myeloid cells results in a type 1 helper T-cell (Th1 cells) response in mice subjected to transverse aortic constriction (TAC), characterized by cardiac Th1 infiltration and adhesion to cardiac fibroblasts (CFBs) through vascular adhesion molecule 1 (VCAM-1).<sup>10-12</sup> Further, while T-cell deficient mice, including *Tcra*<sup>-/-</sup> or *MhcII*<sup>-/-</sup>, are protected from cardiac fibrosis in response to

TAC, adoptive transfer of Th1 cells into these mice partially restored cardiac fibrosis.<sup>10,12</sup> This supports that effector T-cells exhibit sustained activation in the cardiac inflammatory environment, directly responding to stimuli induced by TAC. One of such stimuli is the presentation of ROS-induced cardiac neoantigen by antigen presenting cells (APCs), which induces T-cell activation and clonal expansion.<sup>13,14</sup> While we know that this process is potentiated by DAMP-MyD88 signaling in APCs,<sup>9</sup> whether direct effects of DAMPs on T-cells contribute to this response, as well as the T-cell intrinsic mechanisms necessary to prevent their overactivation have yet to be characterized. Thus far, only one study has shown MyD88 to be partially protective in TAC, using global cardiac MyD88 deletion with Adeno-Associated Virus (AAV).<sup>15</sup> While DAMP receptors and MyD88 are predominantly expressed in innate immune cells and provide pro-inflammatory signaling, adaptive immune cells including T-cells express them as well,<sup>16-18</sup> but their function in cardiac inflammation is unknown.

We hypothesized that TCR activated T-cell sensing of DAMPs will activate MyD88 thus contributing to T-cell activation and cardiac fibrosis in response to TAC. To our surprise, this was not the case, and instead we found that MyD88 deletion in T-cells resulted in enhanced T-cell effector function and worsened fibrosis, revealing a novel T-cell intrinsic mechanism that limits TCR overactivation and tunes down inflammation in the onset of experimental HF.

## Methods

### Data Availability:

The data, methods, and materials will be available to other researchers for the purposes of reproducing the results or replicating procedures. Detailed methods and any associated references are provided in the supplementary material.

### Animals:

All animal studies were approved by the Tufts University Institutional Animal Care and Use Committee. C57BL/6, CD45.1<sup>19</sup>, and *Tcra*<sup>-/-</sup> mice<sup>20</sup> were bred and maintained under pathogen free conditions. *Myd88*<sup>-/-</sup> mice<sup>21</sup> were donated by Dr. Linden Hu (Tufts University, Boston MA), and maintained under specific pathogen free conditions as heterozygotes by crossing with C57BL/6J mice. *Myd88*<sup>fl/fl</sup> *CD4*<sup>Cre</sup> mice were generated by crossing *Myd88*<sup>fl/fl</sup> mice<sup>22</sup> with constitutive *CD4*<sup>Cre</sup> expressing mice<sup>23</sup> (Jackson Laboratory). MyD88 excision was determined by PCR (see Supplemental Table 1 for primer sequences).

### Statistical Analysis:

Statistical analysis was performed using GraphPad Prism 9.4.1. All data is presented as mean ± SEM. Normality was assessed using the D'Agostino-Pearson Test or the Shapiro-Wilk Test. For any data that was determined to have a normal distribution, a T-test was used to compare 2 means, or for >2 means a one-way ANOVA with Tukey's multiple comparison test or two-way ANOVA with Sidak's multiple comparison test were used. For data that was determined not have a normal distribution, a Mann-Whitney Test was used to

compare 2 means, or for  $>2$  means a Kruskal-Wallis Test was used with Dunn's multiple comparison test. Exact p values are shown in all graphs. Sample size was determined by power calculation using <http://powerandsamplesize.com/Calculators>.

## Results:

### Adoptive Transfer of *Myd88*<sup>-/-</sup> Th1 cells into *Tcra*<sup>-/-</sup> Mice Induces Greater Cardiac Fibrosis and Systolic Dysfunction than WT Th1 Cells In Response to TAC

We have previously shown that transfer of WT Th1 cells induces cardiac fibrosis in *Tcra*<sup>-/-</sup> mice, otherwise protected from fibrosis and systolic dysfunction in the onset of TAC. Thus, we used this strategy (Figure 1A) to investigate the role of T-cell MyD88 in TAC-induced cardiac remodeling. At 4 weeks post-surgery, we found that *Tcra*<sup>-/-</sup> mice reconstituted with *Myd88*<sup>-/-</sup> Th1 cells had decreased fractional shortening (FS), in contrast to WT Th1 cells, which were unable to alter FS (Figure 1B), as we have previously described.<sup>12</sup> Despite this, both WT and *Myd88*<sup>-/-</sup> Th1 cells induced similar left ventricular hypertrophy, as measured by normalized left ventricular weight (Figure 1C) and wheat-germ agglutinin (WGA) histologic staining (Figure 1D, 1E). Interestingly, we found *Tcra*<sup>-/-</sup> mice reconstituted with *Myd88*<sup>-/-</sup> Th1 cells exhibited significantly greater cardiac fibrosis and cardiac T-cell infiltration compared to mice reconstituted with WT Th1 cells (Figure 1D–1G). Further analysis showed that *Myd88*<sup>-/-</sup> Th1 cells induced higher cardiac transcript of *Col3* and *Tgfb1* after TAC, and a trend upward for *Col1* (Figure 1H–1J). We confirmed equal reconstitution of both WT and *Myd88*<sup>-/-</sup> Th1 cells by flow cytometry quantification of TCR $\beta$ <sup>+</sup>CD4<sup>+</sup> cells, finding similar frequencies in the spleen and mediastinal lymph nodes (mLN) (Figures S1A–C). Together, these data demonstrate that MyD88 deletion in T-cells results in enhanced T-cell cardiotropism and has detrimental consequences in cardiac fibrosis and contractile function.

### Deletion of MyD88 in T-Cells Results in Enhanced Pro-Inflammatory Function

As an initial step to understand the intrinsic role MyD88 might play in cardiac T-cell function, we took an unbiased approach and compared the gene expression profile of WT and *Myd88*<sup>-/-</sup> Th1 cells by bulk RNA-sequencing. We found  $>100$  differentially expressed genes when MyD88 was deleted in T-cells (Figure 2A). Gene set enrichment analysis (GSEA) revealed enriched genes for “MAPK3 Target genes” as well as decreased enrichment in “Apoptosis” and “Negative Regulation of T-cell Mediated Immunity” alongside the expected decreased enrichment for “TLR signaling pathways” (Figure 2B–2E). We validated these pathways at the protein level and found not only increased phosphorylation of the MAPK effectors ERK and p38, but also increased NF- $\kappa$ B and AKT phosphorylation (Figure 2F–2G) in *Myd88*<sup>-/-</sup> compared to WT Th1 cells. Each signal downstream of the TCR, and participate in clonal expansion, T-cell survival, and effector functions. However, we found similar expression of the Th1 signature cytokine, IFN $\gamma$ , and transcription factor, Tbx21, at the protein and transcript level in WT and *Myd88*<sup>-/-</sup> Th1 cells (Figure S2B–S2D). Taken together, these data demonstrate that MyD88 deletion in Th1 cells enhances TCR signaling pathways involved in T-cell activation and survival, supporting an anti-inflammatory role for MyD88 in T-cells, in contrast to its well established pro-inflammatory role in myeloid cells.

## Mouse and Human T-cells Express MyD88 in the Cardiac Inflammatory Environment

We hypothesized that constant stimuli in the cardiac inflammatory environment would require T-cells to have a mechanism controlled by MyD88 to limit T-cell overactivation. We found that MyD88 protein levels were increased in the LV of TAC mice compared to sham mice, however the parallel but less frequently used DAMP adaptor TRIF showed no changes in TAC vs. sham hearts (Figure 2H–2I). As this readout includes all cardiac cell types, we then turned to the existing single cell data collected from cardiac leukocytes isolated from sham and TAC hearts<sup>24</sup> to analyze the expression of MyD88 specifically in T-cells. We first re-clustered cardiac CD45<sup>+</sup> cells to include only T-cells in both Sham and TAC mice 1 and 4 weeks post-surgery (Figure 2J–2K, Figure S3) and found that at 1 week post TAC surgery CD4<sup>+</sup>MyD88-expressing cells began to infiltrate the heart, and by 4 weeks post-surgery the number of T-cells expressing *Myd88* was overall increased compared to Sham, as well as their relative expression of *Myd88* (Figure 2L, Figure S3). We then utilized published CITE-seq data<sup>25</sup> from human donors without HF and patients with HF to select T-cell subsets. Using RNA and protein markers, we annotated distinct T-cell states and found evidence of cardiac inflammation including a significant population of MyD88-expressing T-cells in failing hearts (Figure 2M–2N). These data demonstrate that pro-inflammatory T-cells in mice and humans express MyD88 in the setting of cardiac inflammation and suggest a novel role for T-cell MyD88 in limiting the overactivation of T-cells in the inflamed heart.

## T-cell MyD88 Deletion Results in Increased Adhesion to ICAM-1 and VCAM-1 and Primary Cardiac Endothelial Cells

As we observed increased cardiac infiltration of *Myd88*<sup>-/-</sup> Th1 cells compared to WT cells, we then sought to investigate whether MyD88 modulates T-cell interactions with adhesion molecules expressed by the inflamed endothelium required for T-cell extravasation. We used PMA to mimic TCR signaling and induce T-cell integrin activation to enhance adhesion to ICAM-1 and VCAM-1 under shear flow conditions. As expected, there was little adhesion to both ligands in the absence of PMA. However upon PMA treatment, higher numbers of *Myd88*<sup>-/-</sup> Th1 cells bound to both ICAM-1 and VCAM-1 compared to WT Th1 cells (Figure 3A–3D). Adhesion was completely abrogated in the presence of anti-LFA-1 or anti-VLA-4 antibodies, the respective ligands of ICAM-1 and VCAM-1, demonstrating the increased adhesion of *Myd88*<sup>-/-</sup> Th1 cells occurred through canonical interactions (Figure 3A–3D). Further, we did not observe any difference in the surface expression of LFA-1 and VLA-4 between WT and *Myd88*<sup>-/-</sup> Th1 cells (Figure 3E–3F). These data support that MyD88 regulates the integrin activation status downstream of TCR signaling, rather than at the expression level, to modulate T-cell adhesion.

*Myd88*<sup>-/-</sup> Th1 cells also adhered to primary cardiac endothelial cells in higher numbers compared to WT Th1 cells (Figure 3G–3H). However, despite the increased adhesion, the frequency of Th1 cells that transmigrated across the endothelial cells was similar between genotypes (Figure 3I). Because Th1 cell TEM requires chemokine signals for integrin activation, and the CXCL10-Th1 axis is central to T-cell cardiotropism in response to TAC<sup>26,27</sup>, we next evaluated T-cell chemotaxis in response to CXCL10. We found no differences between WT and *Myd88*<sup>-/-</sup> Th1 cell migration (Figure S4A) or in the expression

of the CXCL10 receptor CXCR3 by flow cytometry or western blot (Figure S4B–S4D). These data support that MyD88 regulates T-cell effector function by modulating signals downstream of the TCR that lead to T-cell adhesion to endothelial cells.

### T-cell MyD88 Deletion Results in Enhanced Th1 Cell Adhesion to Cardiac Fibroblast and Cardiac Fibroblast Transformation

Based on the high affinity for VCAM-1 that *Myd88*<sup>-/-</sup> Th1 cells displayed, and knowing that Th1 cells interact with CFB through the VLA-4/VCAM-1 interaction to induce myofibroblast transformation<sup>12</sup>, we next investigated if T-cell MyD88 modulates CFB transformation through adhesion to VCAM-1. We co-cultured primary CFB with WT and *Myd88*<sup>-/-</sup> Th1 cells and detached the adhered T-cells to analyze CFB activation in isolation (Figure 4A). We found that fibroblasts that had been in contact with *Myd88*<sup>-/-</sup> Th1 cells expressed higher levels of alpha-smooth muscle actin ( $\alpha$ SMA) and Collagen type 1, readouts of myofibroblast transformation, compared to those that had been in contact with WT Th1 cells (Figure 4B–4D). As expected, WT Th1 cells adhered to CFB and induced  $\alpha$ SMA expression, however, *Myd88*<sup>-/-</sup> Th1 cells adhered in higher numbers to CFB and induced greater levels of  $\alpha$ SMA compared to WT Th1 cells (Figure 4E–4G). Alteration of Th1:CFB ratio further demonstrated that WT and *Myd88*<sup>-/-</sup> Th1 cells adhered to and induced  $\alpha$ SMA in CFB in a T cell dose dependent manner, with sustained enhancement of *Myd88*<sup>-/-</sup> Th1 cell adhesion and CFB transformation at all ratios (Figure S5). Moreover, inhibition of either the VLA-4/VCAM-1 interaction or TGF $\beta$  blunted myofibroblast transformation by both genotypes, and the former blocked all T-cell adhesion, confirming that increased myofibroblast transformation induced by *Myd88*<sup>-/-</sup> T cells occurred through contact-dependent induction of TGF $\beta$  (Figure 4E–4G). These data demonstrate that the enhanced binding of *Myd88*<sup>-/-</sup> Th1 cells to CFB VCAM-1 results in increased CFB transformation in a TGF $\beta$ -dependent manner, a plausible mechanism to enhance cardiac fibrosis during TAC.

### MyD88 Modulates T-Cell Activation through TCR Signaling

Based on our findings demonstrating overall improved T-cell effector function in the absence of MyD88, we then sought to dissect if MyD88 in T-cells modulated T-cell activation through DAMP receptors (TLRs/IL-1R) or through the TCR. We first found that relevant DAMPs which signal through MyD88 such as pro-IL-1 $\beta$ , IL-33, and HMGB1 were increased at the protein level in the LV of WT mice subjected to TAC compared to sham mice (Figure S6A–6B). We then took TCR-activated Th1 cells, removed them from TCR stimulation, and treated them with cardiac lysate from TAC mice (containing DAMPs) to test whether cardiac DAMPs can further activate T-cells in the absence of TCR signals. Cardiac DAMPs, or purified HMGB1 alone, were not sufficient to induce the expression of the T-cell activation markers CD69 and CD25 (Figure 5A–5C, S6C–S6E). However, the same dose of cardiac DAMPs was able to increase MHCII expression in dendritic cells (Figure 5D–5E). To ensure that canonical DAMP signaling was functional in T-cells despite measuring low receptor expression (Figure S6F–S6G), we treated WT and *Myd88*<sup>-/-</sup> Th1 cells with LPS, a TLR4 ligand that signals through MyD88, and found LPS induced a MyD88-dependent increase in ERK phosphorylation and IL-6 expression (Figure S6H–S6J), both downstream of MyD88. These data demonstrate that despite a functional



TLR-MyD88 axis in T-cells, signals through this pathway do not further induce CD69 or CD25 expression, prompting us to explore whether MyD88 modulation of T-cell activation occurs downstream of the TCR.

To do so, we measured phospho-ZAP70, a component of the TCR signaling complex that marks T-cell activation, using TCR stimulation *in vitro* using  $\alpha$ CD3/ $\alpha$ CD28, and found that *Myd88*<sup>-/-</sup> Th1 cells exhibited higher expression of pZAP70 compared to WT after activation but not at baseline (Figure 5F–5G). Additionally, TCR activation of *Myd88*<sup>-/-</sup> Th1 cells resulted in higher levels of CD69 (Figure 5H–5I), and increased secretion of the cytokines IL-2 and TNF $\alpha$  compared to WT Th1 cells (Figure 5J–5K), confirming an overall enhanced activation status in *Myd88*<sup>-/-</sup> Th1 cells. Further, small molecule inhibition of MyD88 during T-cell activation in WT Th1 cells recapitulated both increased CD69 and pZAP70 (Figure S7). Interestingly, TCR activation of WT cells correlated with upregulation of MyD88 protein expression compared to inactivated cells, directly associating MyD88 expression with TCR signaling for the first time (Figure 5L–5M). To further investigate how MyD88 modulates T-cell activation, we investigated the localization of MyD88 upon TCR engagement by immunofluorescence. We again confirmed increased expression of MyD88 upon TCR activation, alongside expected puncta of TCR $\beta$  clusters at the membrane during TCR-induced activation.<sup>28</sup> Strikingly, specific MyD88 signal colocalized in said TCR $\beta$  puncta (Figure 5N–5O), and when T-cells were removed from TCR stimulation, MyD88 decreased at the membrane along with clustered TCR $\beta$ , albeit not back to the level of naïve T-cells. Interestingly, using confocal microscopy we found MyD88 to co-localize with TCR $\beta$  in multiple planes close and distal to the TCR engagement, and MyD88 was also found in isolation far from TCR engagement (Figure S8). Together, these data demonstrate that MyD88 co-localizes with the TCR at the membrane during TCR engagement and suggests that MyD88 functions as a brake of T-cell activation downstream of the TCR rather than through TLR-DAMP signaling.

### MyD88 Deletion Enhances T-Cell Survival:

As TCR signaling leads to optimal T-cell proliferation and survival, we next investigated the role of T-cell MyD88 in T-cell survival as another mechanism to explain increased cardiac T-cell presence, and therefore increased fibrosis. Th1 cells were cultured in the absence of TCR engagement or cytokine stimulation as a way to induce steady T-cell death, and imaged in real time (Figure 6A). Interestingly, *Myd88*<sup>-/-</sup> Th1 cells exhibited decreased cell death over time compared to WT Th1 cells, a finding which was further exacerbated by serum starvation (Figure 6A–6B). Moreover, we performed *in vivo* competitive survival experiments using equal numbers of adoptively transferred WT and *Myd88*<sup>-/-</sup> Th1 cells, carrying the CD45.1 and CD45.2 alleles respectively, into healthy *Tcra*<sup>-/-</sup> recipient mice (Figure 6C). We found that as early as 1 week post transfer, there were higher numbers of *Myd88*<sup>-/-</sup> Th1 cells in the spleen, and this survival advantage was sustained 2 and 4 weeks post transfer (Figure 6D–6E). These data demonstrate a long-term survival benefit *in vivo* for *Myd88*<sup>-/-</sup> Th1 cells compared to WT cells and suggest that MyD88 modulation of T-cell survival in activated T-cells may be responsible for the increased cardiac T-cell presence during TAC.

To distinguish between survival and proliferative cues modulated by MyD88 upon TCR engagement, we next assessed the proliferative capacity of Th1 cells, and found that WT and *Myd88*<sup>-/-</sup> Th1 cells showed similar CFSE dilution as a measurement of proliferation in the presence of IL-2 after 1 and 3 days in culture (Figure 6F–6G). We additionally isolated naïve CD4<sup>+</sup> T-cells from WT and *Myd88*<sup>-/-</sup> mice and traced CFSE dilution as they differentiated into effector T-cells in response to TCR stimulation. We again found rapid but similar proliferation in the presence or absence of MyD88 (Figure 6H–6I). From these data, we conclude that MyD88 acts at the TCR during active TCR signaling and its deficiency results in a T-cell survival advantage that may explain enhanced cardiac inflammation.

### T-cell specific MyD88<sup>-/-</sup> mice develop more cardiac fibrosis and cardiac fibroblast activation

We next generated T-cell specific MyD88<sup>-/-</sup> mice (*Myd88*<sup>fl/fl</sup>*CD4*<sup>Cre</sup>) to investigate the intrinsic role of T-cell MyD88 in T-cell activation and adverse cardiac remodeling in response to TAC. We confirmed that *Myd88*<sup>fl/fl</sup>*CD4*<sup>Cre+</sup> mice had excision of *Myd88* exon 3 and ablated Myd88 protein specifically in T-cells (Figure 7A–7C). In response to TAC, we found higher levels of perivascular and interstitial fibrosis in *Cre*<sup>+</sup> mice (T-MyD88<sup>-/-</sup>) compared to *Cre*<sup>-</sup> littermates (T-MyD88<sup>+/+</sup>), but no baseline differences, suggesting TCR engagement is needed for MyD88 dependent fibrosis (Figure 7D–7F). As observed in our adoptive transfer model, each group of mice developed similar cardiac hypertrophy by LV weight and WGA staining, and neither group developed significant cell death, determined by TUNEL staining (Figure S9). In line with the pro-fibrotic phenotype, we found TAC induced similar increases in *Col1* and *Tgfb1* but greater cardiac expression of *Col3* and *Fn1* (Fibronectin) in T-MyD88<sup>-/-</sup> mice (Figure 7G–7J). Interestingly, we found a significant increase in total MEFSK4<sup>+</sup> CFBs in the hearts of T-MyD88<sup>-/-</sup> but not T-MyD88<sup>+/+</sup> mice in response to TAC (Figure 7K–7L). Further co-staining of αSMA with PDGFRα and CD31 determined that the majority of αSMA<sup>+</sup> cells were also PDGFRα and that PDGFRα<sup>+</sup> αSMA<sup>+</sup> cardiac fibroblasts were increased in TAC T-MyD88<sup>-/-</sup> compared to T-MyD88<sup>+/+</sup> mice (Figure 7M–O). We also observed limited, yet still present, expression of αSMA in CD31<sup>+</sup> vessels (Supplemental Figure 9F). Moreover, to visualize proliferating and non proliferating fibroblasts, we stained with Ki67 and found that while TAC increased the numbers of PDGFRα<sup>+</sup>Ki67<sup>+</sup> cells in both genotypes, T cell MyD88 deficiency did not alter the presence of proliferating fibroblasts at this time point (Figure 7P–7Q, and Supplemental Figure 9G). Together, these confirm that mice deficient in T-cell MyD88 have increased cardiac fibrosis in response to TAC alongside with increased CFB co-expressing αSMA and PDGFRα, yet similar number of proliferating CFBs at this time point.

### T-cell specific MyD88<sup>-/-</sup> mice have increased T-cell cardiac infiltration, TCR activation, and decreased survival to TAC

We next characterized the inflammatory profile of T-MyD88<sup>-/-</sup> mice in response to TAC, finding increased cardiac CD4<sup>+</sup> T-cells compared to T-MyD88<sup>+/+</sup> mice (Figure 8A–8B), however when we quantified effector T-cells (defined as CD62L<sup>lo</sup>CD44<sup>hi</sup>, gating strategy in Figure S10A), we found similar increases in mLN CD4<sup>+</sup> effector T-cells but increased splenic effector T-cells in T-MyD88<sup>-/-</sup> mice, a sign of enhanced systemic inflammation (Figure 8C–8D). Additionally, only T-MyD88<sup>-/-</sup> mice exhibited increased cardiac CD8<sup>+</sup>



T-cells after TAC (Figure S10D). We further quantified CD69 expression in cardiac T cells to probe TCR engagement in the cardiac inflammatory environment and found increased numbers of both CD4<sup>+</sup> and CD8<sup>+</sup> T-cells expressing CD69 in the hearts of T-MyD88<sup>-/-</sup> mice (Figure 8E, Figure S10E). Moreover, splenic CD4<sup>+</sup> T cells from T-MyD88<sup>-/-</sup> mice showed enhanced levels of pZAP70 compared to T-MyD88<sup>+/+</sup> mice in response to TAC, with no differences observed in pZAP70 in sham mice between groups (Figure 8F–8G), demonstrating enhanced TCR activation induced by TAC in T-MyD88<sup>-/-</sup> mice. Despite this, and similar to *in vitro* differentiated Th1 cells, T-cells from T-MyD88<sup>-/-</sup> mice had comparable levels of IFN $\gamma$  to those from MyD88<sup>+/+</sup> control mice in the onset of TAC (Figure 8H–8I). Moreover, T-MyD88<sup>-/-</sup> mice also exhibited increased cardiac CD11b<sup>+</sup>CD11c<sup>+</sup>MHC-II<sup>+</sup> dendritic cells and CD11b<sup>+</sup>CCR2<sup>+</sup>MHC-II<sup>+</sup> myeloid cells, but similar neutrophils (Figure S11A–D), and we did not observe changes in splenic or mediastinal T-regs at baseline or during TAC (Figure S11F–G).

Overall increases in cardiac inflammation co-existed with increased levels of cardiac *Anp* in T-MyD88<sup>-/-</sup> TAC mice compared to T-MyD88<sup>+/+</sup>, suggestive of cardiac damage (Figure 8J). Lastly, the decline in fractional shortening in response to TAC at 4 weeks was comparable between genotypes, despite the increased cardiac fibrosis and inflammation (Figure 8K). However, at 10 weeks post TAC, T-MyD88<sup>-/-</sup> mice had lower fractional shortening compared to T-MyD88<sup>+/+</sup>, demonstrating enhanced systolic decline long term after TAC (Figure 8L). Moreover, survival post TAC was significantly decreased in T-MyD88<sup>-/-</sup> mice compared to T-MyD88<sup>+/+</sup> littermates (Figure 8M). Taken together, T-MyD88<sup>-/-</sup> mice subjected to TAC have unrestrained systemic and cardiac TCR activation characterized by enhanced P-ZAP-70 expression as well as enhanced presence of CD69<sup>+</sup> T cells and MHC-II<sup>+</sup> myeloid cells. This demonstrates a central role for T-cell MyD88 in limiting T-cell activation through the TCR to modulate cardiac inflammation in HF.

## Discussion:

Here we report that deletion of MyD88 in T-cells is detrimental for the heart and for survival in experimental non-ischemic heart failure. We find that Th1 cells, major drivers of cardiac fibrosis in response to TAC, survive longer, are more inflammatory, have enhanced cardiotropism, and greater adhesion to cardiac endothelial cells and fibroblasts when lacking MyD88. We demonstrate for the first time, to our knowledge, the expression of MyD88 in cardiac mouse and human T-cells, and its localization to the TCR upon TCR engagement. Moreover, we show evidence that MyD88 functions as a brake of T-cell activation upon TCR signaling, rather than solely modulating TLR signaling induced by DAMPs, its classical function in innate cells. This represents a novel T-cell modulatory mechanism involved in cardiac inflammation, fibrosis, and dysfunction in experimental HF.

The pro-inflammatory role of MyD88 in myeloid cells is well established. It triggers pro-inflammatory cytokine secretion, and induces the expression of major histocompatibility complex type II (MHC-II) in antigen presenting cells for an optimal T-helper cell immune response.<sup>9</sup> In contrast, its role in adaptive immune cells is not well understood, and even less so in the context of cardiac inflammation. The only study investigating a role for MyD88 in pressure-overload induced HF showed that global cardiac MyD88 deletion conferred a

partial protection in response to TAC. However this used a non-cell specific approach, and therefore protection was likely conferred through inhibition of DAMP signaling in innate immune cells.<sup>15</sup> Our data provide evidence that in contrast to its role in innate immune cells in cardiac inflammation, in T-cells, MyD88 plays an anti-inflammatory role, which we hypothesize contributes to the partial protection was observed with global cardiac MyD88 deletion.

We have previously shown that Th1 cell production of IFN $\gamma$  is essential for the induction of cardiac fibrosis in TAC<sup>12</sup>, therefore we hypothesized that MyD88 might modulate IFN $\gamma$  expression in addition to T-cell activation. However, our findings demonstrate that the lack of MyD88 did not result in changes to Th1 identify, as seen by IFN $\gamma$  or Tbx21 levels in *in vitro* differentiated T cells as well as *in vivo* during TAC. This somewhat differs from a described role for T cell MyD88 in the Th1/Th17 response to LPS injection and ovalbumin (OVA) immunization.<sup>29</sup> Isolated T cells from LPS and OVA treated mice re-stimulated and expanded for OVA *ex vivo* had decreased IFN $\gamma$  and IL-17 expression, despite similar proliferation and T-reg frequency. While the proliferation and T-reg frequency are in line with our results in mice subjected to TAC, the differences in the IFN $\gamma$  response could be attributed to different TCR stimuli *in vitro* (OVA vs anti-CD3/anti-CD28) and different inflammatory conditions *in vivo* (LPS/OVA vs TAC). Moreover, we show that cardiac DAMPs do not further induce activation marker expression on T cells, while LPS, used in that report, is a more potent activator of TLR4. Thus, the context of T-cell activation may differently influence the outcome of MyD88-TCR signaling in these two distinct inflammatory settings. Along these lines, our results demonstrating that MyD88 functions as a brake for T cell effector function is in agreement with studies showing that T-MyD88<sup>-/-</sup> mice had slowed growth of melanoma.<sup>30</sup> When MyD88 was deleted using the *Foxp3* Cre driver, authors reported no difference in T-reg numbers, in line with our results, but worse allograft survival, potentially a result of enhanced T-cell effector function.<sup>31</sup>

While T-cell effector function was broadly enhanced in the absence of MyD88, we mainly found functions regulated directly by TCR signaling to be enhanced in *Myd88*<sup>-/-</sup> Th1 cells. For example, TCR signaling directly influences cytokine secretion, cell survival, and T-cell adhesion,<sup>28</sup> and specifically, p-AKT signaling has been previously shown to regulate integrin activation on T-cells.<sup>32</sup> Thus, we propose that the increased adhesion to protein ligands, endothelial cells, and CFBs observed in *Myd88*<sup>-/-</sup> Th1 cells is a direct result of MyD88 modulation of TCR induced AKT signaling. This is further supported by our *in vitro* studies showing that enhanced adhesion to ICAM-1 and VCAM-1 of *Myd88*<sup>-/-</sup> Th1 cells was dependent on PMA treatment, a mimic of active TCR stimulation known to induce p-AKT. We hypothesize increased T-cell endothelial interaction might further contribute to perivascular fibrosis. On the contrary, the lack of alteration to Th1 polarization or chemotaxis to CXCL10 in *Myd88*<sup>-/-</sup> Th1 cells would be explained by the fact that these two are more dependent on cytokine receptor or G-protein coupled receptor signaling, respectively, both of which operate mostly independently from the TCR.<sup>33,34</sup> Further studies depicting how MyD88 specifically regulates these signals are needed to explain why many, but not all T-cell effector functions are enhanced in *Myd88*<sup>-/-</sup> Th1 cells. TCR signaling is intimately associated with cell survival, and as such, we found that *Myd88*<sup>-/-</sup> Th1 cells exhibited a survival advantage both *in vivo* and *in vitro*. However, we have yet to fully

elucidate the mechanism of cell death regulated by MyD88, whether that be apoptosis as suggested by our RNA-seq results, or other pathways including inflammatory cell death. In contrast to the survival advantage conferred by MyD88 deletion in T-cells that we outline here, we were surprised to see similar cellular proliferation in response to CD3/CD28 stimulation or IL-2 *in vitro*. While MyD88 might be more specific to pro-survival signaling, it is possible that MyD88 modulates proliferation *in vivo* in a more complex inflammatory environment with DAMPs and TCR co-stimulation.

While we originally thought that sensing of cardiac DAMPs would be a major factor influencing Th1-MyD88 signaling, we found that DAMPs either alone or in combination were unable to modulate T-cell activation *in vitro*. One study has shown a protective role for HMGB1 in TAC, however other studies have disputed this.<sup>35,36</sup> Our RNA-seq data and *in vitro* studies stimulating T-cells with cardiac lysate and DAMPs suggest that this is not the case during sterile inflammation in the heart. Our results demonstrate that the absence of MyD88 alters T-cell effector function in response to TCR engagement and in the absence of TLR stimulation *in vitro*. Additionally, it has been well described that TLR ligation can act as a co-stimulatory signal for T-cell activation and influence T-cell polarization.<sup>37,38</sup> While we did not explicitly test this, it is possible that in a more complex scenario *in vivo*, DAMP agonism of TLRs in Th1 cells among other cells also contribute to cardiac fibrosis and inflammation, in line with studies reporting that DAMP sensing by CFB can contribute to fibrosis.<sup>39,40</sup> More work in the field is warranted to investigate potential crosstalk between TLR / DAMP receptors and TCR signals through MyD88 or other adaptors in distinct inflammatory and infectious settings.

To our knowledge, this is the first investigation of a T-cell specific deletion for MyD88 in sterile cardiac inflammation, which we characterized using both adoptive transfer and endogenous genetic deletion. In the T-MyD88<sup>-/-</sup> mouse, we found no baseline changes in cardiac function or T-cell subsets in the heart and lymphoid organs, and no baseline expression of P-ZAP70 in T cells, immediately downstream TCR engagement. The increased phosphorylation of ZAP-70 in T-MyD88<sup>-/-</sup> mice compared to T-MyD88<sup>+/+</sup> control littermates in the onset of TAC further support that MyD88 modulates T-cell cardiac inflammation through TCR mediated activation secondary to cardiac insult, rather than non-specific DAMP induced signals. One limitation of this mouse model is that the CD4-Cre driver also excises MyD88 from double positive CD4/CD8 T-cells during thymic development, thus MyD88 is also deleted in CD8<sup>+</sup> T-cells. And indeed, we found increases in CD8<sup>+</sup>CD69<sup>+</sup> T-cells in the heart. Our adoptive transfer approach of Th1 cells into T-cell deficient mice eliminates any confounding effects from other T-cell subtypes, and in fact showed earlier systolic decline than the T-MyD88<sup>-/-</sup> mice post TAC. Moreover, our observation that T-MyD88<sup>-/-</sup> mice have worsened survival to TAC further emphasizes the necessity of T-cell MyD88 in limiting chronic inflammation in HF in the context of a fully intact immune system.

Both our adoptive transfer and genetic approach for MyD88 deletion in T-cells showed significantly increased cardiac fibrosis, which we attribute to increased T-cell survival and enhanced fibroblast activation. We have previously shown that CD4 cells co-localize with CFB *in vivo*<sup>13</sup> and that their contact is required for myofibroblast transformation *in vitro*.<sup>12</sup>

As such, we conclude while IFN $\gamma$  was not enhanced on a per cell basis, the overall increased presence of highly inflammatory T-cells resulted in greater T-cell fibroblast cross-talk and as such, greater fibrosis. Moreover, our findings in T-MyD88<sup>-/-</sup> mice provide evidence that the fibrotic response resulting by the lack of MyD88 in T cells is in part due to overactivated CD4<sup>+</sup> and CD8<sup>+</sup> T cells unable to tune down TCR signals, as seen by increased P-ZAP70 and CD69. However enhanced T-cell function further contributed to an overall increased proinflammatory and profibrotic milieu consisting of increased MHC-II<sup>+</sup> myeloid cells, able to continue to reactivate T-cells. Together, this potent inflammatory environment increased fibrosis. While to thoroughly determine whether T-cell MyD88 modulates CFB proliferation and/or myofibroblast transformation, Periostin-Cre lineage tracing would be required,<sup>41,42</sup> our results suggest that the lack of MyD88 in T cells results in enhanced CFB activation given the increased presence of PDGFR $\alpha$ <sup>+</sup>  $\alpha$ SMA<sup>+</sup> CFBs, rather than increased proliferation at this time post TAC. It is possible that T-cell MyD88 modulates CFB proliferation at earlier time points post TAC<sup>43</sup> and thus we see more total activated CFBs at this time point. Nevertheless, the increased T cell activation and survival of MyD88<sup>-/-</sup> T cells results in a heightened fibrotic response dependent on TGF $\beta$ , collagen III and fibronectin. It is further plausible that enhanced binding by MyD88<sup>-/-</sup> Th1 cells increases fibroblast transformation due to stronger collective mechanical force, and while we did not explicitly test this, future studies aim to further define mechanisms of T-cell CFB interaction.

Despite these interesting and novel findings, our study has some limitations we would like to outline. Given the altered fibrotic response and the worsened survival to cardiac stress observed in the absence of T-cell MyD88, one can speculate that cardiac stiffness may lead to diastolic dysfunction and contributes to less survival to TAC, in addition to the systolic dysfunction we report, yet we have not performed hemodynamics studies to thoroughly characterize the role of T-cell MyD88 in cardiac relaxation. While we demonstrate a modulatory role for T-cell MyD88 in pressure overload HF, this role may be different in other models of sterile or infectious inflammation. We focus on Th1 cells, but our data indicate that MyD88 might contribute similarly to CD8<sup>+</sup> T-cell activation, which has other implications in contexts more dependent on a cytotoxic T-cell response, such as cancer or immune checkpoint-induced myocarditis.<sup>44,45</sup> Mechanistically, while we demonstrate the first evidence that MyD88 co-localizes with the TCR during active TCR engagement and modulates immediate downstream signals such as ZAP70 and AKT, the exact molecular binding partner(s) that recruit or limit MyD88 access to the TCR signaling complex to modulate T-cell activation remain an ongoing area of investigation. We hypothesize that the strength of TCR stimulation alongside other signals that recruit MyD88 will influence the degree of MyD88 localization to the TCR vs. other locations or outcomes.

The different role we report for MyD88 in T-cells vs. innate immune cells in the context of DAMP signals might explain the limited efficacy of clinical trials targeting DAMPs such as IL-1 $\beta$ , whereas a more targeted approach modulating the signaling effectors such as MyD88 might prove more effective<sup>2,46</sup>

## Conclusion:

In summary, we report here a novel role for MyD88 in regulating T-cell signaling and effector function in the context of cardiac inflammation and cardiac fibrosis. This work contributes to our understanding of cardiac inflammation in HF and reveals a unique cell-intrinsic role for MyD88 in modulating TCR signaling that is independent of T-cell TLR recognition of DAMPs. This novel anti-inflammatory role for MyD88, distinct from the pro-inflammatory role in innate immunity, is a necessary mechanism to limit T-cell overactivation and survival in response to cardiac stress. Our results highlight the importance of cell specific therapeutic approaches for immunomodulation in HF.

## Supplementary Material

Refer to Web version on PubMed Central for supplementary material.

## Acknowledgements

Additional thanks to Albert Tai at Tufts University for help in analyzing bulk RNA-seq data, and the Poltorak lab for assistance with *in vitro* cell death assays. Biorender was used to generate figures.

## Funding:

This work was supported by National Institute of Health (NIH) Grants R01 HL123658 and R01 HL144477 (P.A.), American Heart Association (AHA) Pre-Doctoral Fellowship 906361 (A.L.B.), NIH F30 Grant HL162200 (A.L.B.), F31 Grant HL159907A (S.S.), and NIH F31 Grant HL140883 (N.N.), and AHA Pre-Doctoral Fellowship 826325 (J.M.A). K.L is supported by: NIH Grants P30AR073752, R01 HL138466, R01 HL139714, R01 HL151078, R01 HL161185, and R35 HL161185, Leducq Foundation Network (#20CVD02), Burroughs Wellcome Fund (1014782), and Children's Discovery Institute of Washington University and St. Louis Children's Hospital (CH-II-2015-462, CH-II-2017-628, PM-LI-2019-829), Foundation of Barnes-Jewish Hospital (8038-88), and generous gifts from Washington University School of Medicine. S.S. and K.S. are supported by R01 AI142005-01.

## Non-Standard Abbreviations:

<b>APCs</b>	Antigen Presenting Cells
<b>CFSE</b>	Carboxyfluorescein Succinimidyl Ester
<b>CITE-seq</b>	Cellular indexing of transcriptomes and epitopes by sequencing
<b>CFB</b>	Cardiac fibroblast
<b>DAMPs</b>	Damage associated molecular patterns
<b>FS</b>	Fractional shortening
<b>GSEA</b>	Gene set enrichment analysis
<b>HF</b>	Heart Failure
<b>HMGB1</b>	High mobility group box 1
<b>ICAM1</b>	Intracellular Adhesion Molecule 1
<b>LPS</b>	Lipopolysaccharide

<b>MHC-II</b>	major histocompatibility complex type II
<b>mLN</b>	mediastinal lymph nodes
<b>MyD88</b>	Myeloid Differentiation Response 88
<b>ROS</b>	Reactive oxygen species
<b>TAC</b>	Transverse Aortic Constriction
<b>TEM</b>	Transendothelial Migration
<b>TCR</b>	T-cell receptor
<b>Th1</b>	Type 1 helper T-cell
<b>TLRs</b>	Toll-like receptors
<b>VCAM1</b>	Vascular Adhesion Molecule 1
<b>WGA</b>	Wheat germ agglutinin

## References:

- Smolgovsky S, Ibeh U, Tamayo TP, Alcaide P. Adding Insult to Injury - Inflammation at the Heart of Cardiac Fibrosis. *Cell. Signal* 2021;77:109828. [PubMed: 33166625]
- Ridker PM, Everett BM, Thuren T, MacFadyen JG, Chang WH, Ballantyne C, Fonseca F, Nicolau J, Koenig W, Anker SD, et al. Antiinflammatory Therapy with Canakinumab for Atherosclerotic Disease. *N. Engl. J. Med* 2017;377:1119–1131. [PubMed: 28845751]
- Chung Eugene S., Packer Milton, Lo Kim Hung, Fasanmade Adedigbo A., Willerson James T. Randomized, Double-Blind, Placebo-Controlled, Pilot Trial of Infliximab, a Chimeric Monoclonal Antibody to Tumor Necrosis Factor- $\alpha$ , in Patients With Moderate-to-Severe Heart Failure. *Circulation*. 2003;107:3133–3140. [PubMed: 12796126]
- Yang D, Han Z, Oppenheim JJ. ALARMINs AND IMMUNITY. *Immunol. Rev* 2017;280:41–56. [PubMed: 29027222]
- Mann DL. Innate Immunity and the Failing Heart. *Circ. Res* 2015;116:1254–1268. [PubMed: 25814686]
- Zhang L, Liu M, Jiang H, Yu Y, Yu P, Tong R, Wu J, Zhang S, Yao K, Zou Y, et al. Extracellular high-mobility group box 1 mediates pressure overload-induced cardiac hypertrophy and heart failure. *J. Cell. Mol. Med* 2016;20:459–470. [PubMed: 26647902]
- Suetomi T, Willeford A, Brand CS, Cho Y, Ross RS, Miyamoto S, Brown JH. Inflammation and NLRP3 inflammasome activation initiated in response to pressure overload by CaMKII $\delta$  signaling in cardiomyocytes are essential for adverse cardiac remodeling. *Circulation*. 2018;138:2530–2544. [PubMed: 30571348]
- Cohen P The TLR and IL-1 signalling network at a glance. *J. Cell Sci* 2014;127:2383–2390. [PubMed: 24829146]
- Deguine J, Barton GM. MyD88: a central player in innate immune signaling. *F1000Prime Rep*. [Internet]. 2014;6. Available from: <https://www.ncbi.nlm.nih.gov/pmc/articles/PMC4229726/>
- Nevers Tania, Salvador Ane M., Grodecki-Pena Anna, Knapp Andrew, Velázquez Francisco, Aronovitz Mark, Kapur Navin K., Karas Richard H., Blanton Robert M., Alcaide Pilar. Left Ventricular T-Cell Recruitment Contributes to the Pathogenesis of Heart Failure. *Circ. Heart Fail* 2015;8:776–787. [PubMed: 26022677]
- Fanny Laroumanie, Victorine Douin-Echinard, Joffrey Pozzo, Olivier Lairez, Florence Tortosa, Claire Vinel, Christine Delage, Denis Calise, Marianne Dutaur, Angelo Parini, et al. CD4+ T Cells



Promote the Transition From Hypertrophy to Heart Failure During Chronic Pressure Overload. *Circulation*. 2014;129:2111–2124. [PubMed: 24657994]

12. Nevers T, Salvador AM, Velazquez F, Ngwenyama N, Carrillo-Salinas FJ, Aronovitz M, Blanton RM, Alcaide P. Th1 effector T cells selectively orchestrate cardiac fibrosis in nonischemic heart failure. *J. Exp. Med* 2017;214:3311–3329. [PubMed: 28970239]
13. Ngwenyama Njabulo, Kirabo Annet, Aronovitz Mark, Velázquez Francisco, Carrillo-Salinas Francisco, Salvador Ane M., Nevers Tania, Amarnath Venkataraman, Tai Albert, Blanton Robert M., et al. Isolevuglandin-Modified Cardiac Proteins Drive CD4+ T Cell Activation in the Heart and Promote Cardiac Dysfunction. *Circulation* [Internet]. 0. Available from: <https://www.ahajournals.org/doi/abs/10.1161/CIRCULATIONAHA.120.051889>
14. Ngwenyama N, Kaur K, Bugg D, Theall B, Aronovitz M, Berland R, Panagiotidou S, Genco C, Perrin MA, Davis J, et al. Antigen presentation by cardiac fibroblasts promotes cardiac dysfunction. *Nat. Cardiovasc. Res* 2022;1:761–774. [PubMed: 36092510]
15. Ha T, Hua F, Li Y, Ma J, Gao X, Kelley J, Zhao A, Haddad GE, Williams DL, Browder IW, et al. Blockade of MyD88 attenuates cardiac hypertrophy and decreases cardiac myocyte apoptosis in pressure overload-induced cardiac hypertrophy in vivo. *Am. J. Physiol.-Heart Circ. Physiol* 2006;290:H985–H994. [PubMed: 16199478]
16. Iwasaki A, Medzhitov R. Toll-like receptor control of the adaptive immune responses. *Nat. Immunol* 2004;5:987–995. [PubMed: 15454922]
17. Reynolds JM, Dong C. Toll-like receptor regulation of effector T lymphocyte function. *Trends Immunol*. 2013;34:511–519. [PubMed: 23886621]
18. Bayer AL, Alcaide P. MyD88: At the heart of inflammatory signaling and cardiovascular disease. *J. Mol. Cell. Cardiol* 2021;161:75–85. [PubMed: 34371036]
19. Mardiney M, Malech HL. Enhanced Engraftment of Hematopoietic Progenitor Cells in Mice Treated With Granulocyte Colony-Stimulating Factor Before Low-Dose Irradiation: Implications for Gene Therapy. *Blood*. 1996;87:4049–4056. [PubMed: 8639760]
20. Mombaerts P, Clarke AR, Rudnicki MA, Iacomini J, Itohara S, Lafaille JJ, Wang L, Ichikawa Y, Jaenisch R, Hooper ML, et al. Mutations in T-cell antigen receptor genes  $\alpha$  and  $\beta$  block thymocyte development at different stages. *Nature*. 1992;360:225–231. [PubMed: 1359428]
21. Adachi O, Kawai T, Takeda K, Matsumoto M, Tsutsui H, Sakagami M, Nakanishi K, Akira S. Targeted Disruption of the MyD88 Gene Results in Loss of IL-1- and IL-18-Mediated Function. *Immunity*. 1998;9:143–150. [PubMed: 9697844]
22. Hou B, Reizis B, DeFranco AL. Toll-like receptor-mediated dendritic cell-dependent and -independent stimulation of innate and adaptive immunity. *Immunity*. 2008;29:272–282. [PubMed: 18656388]
23. Lee PP, Fitzpatrick DR, Beard C, Jessup HK, Lehar S, Makar KW, Pérez-Melgosa M, Sweetser MT, Schlissel MS, Nguyen S, et al. A Critical Role for Dnmt1 and DNA Methylation in T Cell Development, Function, and Survival. *Immunity*. 2001;15:763–774. [PubMed: 11728338]
24. Martini E, Kunderfranco P, Peano C, Carullo P, Cremonesi M, Schorn T, Carriero R, Termanini A, Colombo FS, Jachetti E, et al. Single-Cell Sequencing of Mouse Heart Immune Infiltrate in Pressure Overload–Driven Heart Failure Reveals Extent of Immune Activation. *Circulation*. 2019;140:2089–2107. [PubMed: 31661975]
25. Amrute JM, Luo X, Penna V, Bredemeyer A, Yamawaki T, Heo GS, Shi S, Koenig A, Yang S, Kadyrov F, et al. Targeting the Immune-Fibrosis Axis in Myocardial Infarction and Heart Failure [Internet]. 2022 [cited 2022 Nov 21];2022.10.17.512579. Available from: <https://www.biorxiv.org/content/10.1101/2022.10.17.512579v1>
26. Ngwenyama N, Salvador AM, Velázquez F, Nevers T, Levy A, Aronovitz M, Luster AD, Huggins GS, Alcaide P. CXCR3 regulates CD4+ T cell cardiotropism in pressure overload–induced cardiac dysfunction. *JCI Insight* [Internet]. 4. Available from: <https://www.ncbi.nlm.nih.gov/pmc/articles/PMC6483643/>
27. Piali L, Weber C, LaRosa G, Mackay CR, Springer TA, Clark-Lewis I, Moser B. The chemokine receptor CXCR3 mediates rapid and shear-resistant adhesion-induction of effector T lymphocytes by the chemokines IP10 and Mig. *Eur. J. Immunol* 1998;28:961–972. [PubMed: 9541591]

28. Yi J, Balagopalan L, Nguyen T, McIntire KM, Samelson LE. TCR microclusters form spatially segregated domains and sequentially assemble in calcium-dependent kinetic steps. *Nat. Commun* 2019;10:277. [PubMed: 30655520]
29. Schenten D, Nish SA, Yu S, Yan X, Lee HK, Brodsky I, Paskan L, Yordy B, Wunderlich FT, Brüning JC, et al. Signaling through the Adaptor Molecule MyD88 in CD4+ T Cells Is Required to Overcome Suppression by Regulatory T Cells. *Immunity*. 2014;40:78–90. [PubMed: 24439266]
30. Cataisson C, Salcedo R, Michalowski AM, Klosterman M, Naik S, Li L, Pan MJ, Sweet A, Chen J-Q, Kostecka LG, et al. T-Cell Deletion of MyD88 Connects IL17 and  $\text{I}\kappa\text{B}\zeta$  to RAS Oncogenesis. *Mol. Cancer Res* 2019;17:1759–1773. [PubMed: 31164412]
31. Borges CM, Reichenbach DK, Kim BS, Misra A, Blazar BR, Turka LA. T Regulatory Cell Expressed Myd88 Is Critical For Prolongation Of Allograft Survival. *Transpl. Int. Off. J. Eur. Soc. Organ Transplant* 2016;29:930–940.
32. Johansen KH, Golec DP, Thomsen JH, Schwartzberg PL, Okkenhaug K. PI3K in T Cell Adhesion and Trafficking. *Front. Immunol* [Internet]. 2021 [cited 2022 Apr 10];12. Available from: <https://www.frontiersin.org/article/10.3389/fimmu.2021.708908>
33. Groom JR, Luster AD. CXCR3 in T cell function. *Exp. Cell Res* 2011;317:620–631. [PubMed: 21376175]
34. Wojno EDT, Hunter CA, Stumhofer JS. The Immunobiology of the Interleukin-12 Family: Room for Discovery. *Immunity*. 2019;50:851–870. [PubMed: 30995503]
35. Funayama A, Shishido T, Netsu S, Narumi T, Kadowaki S, Takahashi H, Miyamoto T, Watanabe T, Woo C-H, Abe J, et al. Cardiac nuclear high mobility group box 1 prevents the development of cardiac hypertrophy and heart failure. *Cardiovasc. Res* 2013;99:657–664. [PubMed: 23708738]
36. Lin H, Shen L, Zhang X, Xie J, Hao H, Zhang Y, Chen Z, Yamamoto H, Liao W, Bin J, et al. HMGB1-RAGE Axis Makes No Contribution to Cardiac Remodeling Induced by Pressure-Overload. *PLOS ONE*. 2016;11:e0158514. [PubMed: 27355349]
37. Jin B, Sun T, Yu X-H, Yang Y-X, Yeo AET. The Effects of TLR Activation on T-Cell Development and Differentiation [Internet]. *Clin. Dev. Immunol* 2012 [cited 2021 Mar 2]; Available from: <https://www.hindawi.com/journals/jir/2012/836485/>
38. Rahman AH, Taylor DK, Turka LA. The contribution of direct TLR signaling to T cell responses. *Immunol. Res* 2009;45:25–36. [PubMed: 19597998]
39. Turner NA. Inflammatory and fibrotic responses of cardiac fibroblasts to myocardial damage associated molecular patterns (DAMPs). *J. Mol. Cell. Cardiol* 2016;94:189–200. [PubMed: 26542796]
40. Theall B, Alcaide P. The heart under pressure: immune cells in fibrotic remodeling. *Curr. Opin. Physiol* 2022;25:100484. [PubMed: 35224321]
41. Kanisicak O, Khalil H, Ivey MJ, Karch J, Maliken BD, Correll RN, Brody MJ, J Lin S-C, Aronow BJ, Tallquist MD, et al. Genetic lineage tracing defines myofibroblast origin and function in the injured heart. *Nat. Commun* 2016;7:12260. [PubMed: 27447449]
42. Reichardt IM, Robeson KZ, Regnier M, Davis J. Controlling Cardiac Fibrosis Through Fibroblast State Space Modulation. *Cell. Signal* 2021;79:109888. [PubMed: 33340659]
43. Ivey MJ, Kuwabara JT, Pai JT, Moore RE, Sun Z, Tallquist MD. Resident fibroblast expansion during cardiac growth and remodeling. *J. Mol. Cell. Cardiol* 2018;114:161–174. [PubMed: 29158033]
44. Farhood B, Najafi M, Mortezaee K. CD8+ cytotoxic T lymphocytes in cancer immunotherapy: A review. *J. Cell. Physiol* 2019;234:8509–8521. [PubMed: 30520029]
45. Axelrod ML, Meijers WC, Screever EM, Qin J, Carroll MG, Sun X, Tannous E, Zhang Y, Sugiura A, Taylor BC, et al. T cells specific for  $\alpha$ -myosin drive immunotherapy-related myocarditis. *Nature*. 2022;611:818–826. [PubMed: 36385524]
46. Abbate A, Kontos MC, Grizzard JD, Biondi-Zoccai GGL, Van Tassell BW, Robati R, Roach LM, Arena RA, Roberts CS, Varma A, et al. Interleukin-1 Blockade With Anakinra to Prevent Adverse Cardiac Remodeling After Acute Myocardial Infarction (Virginia Commonwealth University Anakinra Remodeling Trial [VCU-ART] Pilot Study). *Am. J. Cardiol* 2010;105:1371–1377.e1. [PubMed: 20451681]

47. Richards DA, Aronovitz MJ, Calamaras TD, Tam K, Martin GL, Liu P, Bowditch HK, Zhang P, Huggins GS, Blanton RM. Distinct Phenotypes Induced by Three Degrees of Transverse Aortic Constriction in Mice. *Sci. Rep* 2019;9:5844. [PubMed: 30971724]
48. Carrillo-Salinas FJ, Anastasiou M, Ngwenyama N, Kaur K, Tai A, Smolgovsky SA, Jetton D, Aronovitz M, Alcaide P. Gut dysbiosis induced by cardiac pressure overload enhances adverse cardiac remodeling in a T cell-dependent manner. *Gut Microbes*. 2020;12:1823801. [PubMed: 33103561]
49. Kaur K, Velázquez FE, Anastasiou M, Ngwenyama N, Smolgovsky S, Aronovitz M, Alcaide P. Sialomucin CD43 Plays a Deleterious Role in the Development of Experimental Heart Failure Induced by Pressure Overload by Modulating Cardiac Inflammation and Fibrosis. *Front. Physiol* [Internet]. 2021 [cited 2022 Nov 5];12. Available from: <https://www.frontiersin.org/articles/10.3389/fphys.2021.780854>
50. Hao Y, Hao S, Andersen-Nissen E, Mauck WM, Zheng S, Butler A, Lee MJ, Wilk AJ, Darby C, Zager M, et al. Integrated analysis of multimodal single-cell data. *Cell*. 2021;184:3573–3587.e29. [PubMed: 34062119]
51. Anastasiou M, Newton GA, Kaur K, Carrillo-Salinas FJ, Smolgovsky SA, Bayer AL, Ilyukha V, Sharma S, Poltorak A, Luscinskas FW, et al. Endothelial STING controls Tcell transmigration in an IFN-I dependent manner. *JCI Insight* [Internet]. 2021 [cited 2021 Jul 29]; Available from: [https://insight.jci.org/articles/view/149346?utm\\_source=TrendMD&utm\\_medium=cpc&utm\\_campaign=JCI\\_Insight\\_TrendMD\\_1](https://insight.jci.org/articles/view/149346?utm_source=TrendMD&utm_medium=cpc&utm_campaign=JCI_Insight_TrendMD_1)

**Novelty and Significance:****What is Known:**

- Helper T-cells are a driving factor of cardiac inflammation and fibrosis in pressure overload HF
- DAMPs induced in HF drive pro-inflammatory signaling in innate immune cells

**What New Information Does this Article Contribute:**

- An intrinsic role for T-cell MyD88 modulates TCR signaling independently of T-cell TLR recognition of cardiac DAMPs and limits T-cell overactivation in response to cardiac stress.
- MyD88 is expressed in mouse and human cardiac infiltrated T-cells.
- T-cell deletion of MyD88 results in enhanced cardiac T-cell infiltration, fibrosis, systolic dysfunction, and worse survival in response to pressure overload induced HF.

**Novelty and Significance:**

Cardiac and systemic inflammation are hallmarks of heart failure, however thus far anti-inflammatory therapies have shown limited success. T-cells, myeloid cells, and damage associated molecular patterns (DAMPs), co-exist in the failing heart. Myeloid cells recognize DAMPs, which signal to converge on the adaptor MyD88, a necessary step for myeloid cell activation and presentation of antigens to CD4<sup>+</sup> T-cells. Little is known about if T-cells can respond directly to cardiac DAMPs, or if there are intrinsic T-cell mechanisms to limit T-cell overactivation. We show that MyD88 is expressed in cardiac T-cells in pre-clinical and clinical heart failure. We report the first evidence, to our knowledge, that T-cell MyD88 limits T-cell activation through T-cell receptor signals, and thus plays an anti-inflammatory role that tunes down cardiac inflammation. As such, *Myd88*<sup>-/-</sup> T-cells exhibit increased pro-inflammatory signaling and effector function *in vitro* and in the onset of heart failure *in vivo*. Further, MyD88 T-cell deficient mice exhibited more cardiac fibrosis and had a survival disadvantage to heart failure as a result of unrestrained pro-inflammatory T-cell activation, T-cell survival, and increased cardiac presence that contributes to cardiac fibrosis and inflammation. Together, our findings outline a novel regulatory mechanism for T-cell mediated cardiac inflammation.

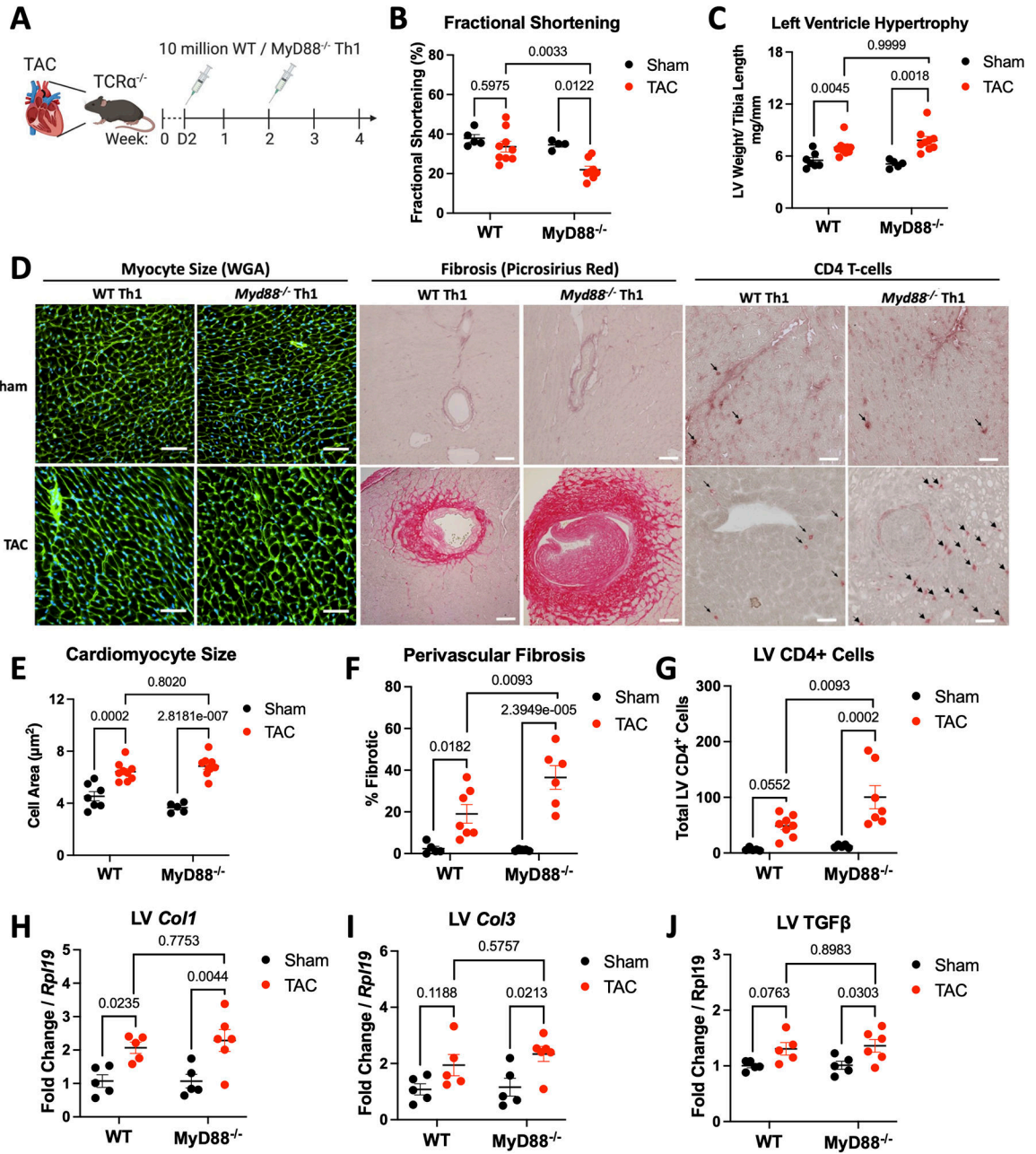


**Figure 1: *Tcrα*<sup>-/-</sup> Mice given *Myd88*<sup>-/-</sup> Th1 cells in the onset of TAC develop more cardiac fibrosis and systolic dysfunction**

A. Schematic of experimental design, 8–10 week old male *Tcrα*<sup>-/-</sup> mice underwent 25G TAC or Sham surgery then were reconstituted with 10 million WT or *Myd88*<sup>-/-</sup> Th1 cells 2 days, then 2 weeks post surgery, and tissues were harvested after 4 weeks. B. Fractional shortening as measured by echocardiography after 4 weeks. C. Measured weight of excised left ventricles normalized to tibia length. D. Representative images of LV of WGA (left), Picrosirius red (middle), and CD4 by IHC (right). Scale bars are 100 μm (middle) or 50 μm (left/right). E. Average cardiomyocyte size quantified using ImageJ on WGA stained sections. F. Left ventricular perivascular fibrosis quantified with ImageJ from Picrosirius



red stained sections. G. CD4 infiltration was counted manually after IHC stain for CD4. H-J. RNA was isolated from the LV of each group of mice for gene expression analysis by RT-qPCR. Each data point is an individual mouse. Statistical analysis by 2-way ANOVA with Sidák's multiple comparison test for all panels except C, which used Kruskal-Wallis test with Dunn's multiple comparison test. P values shown.

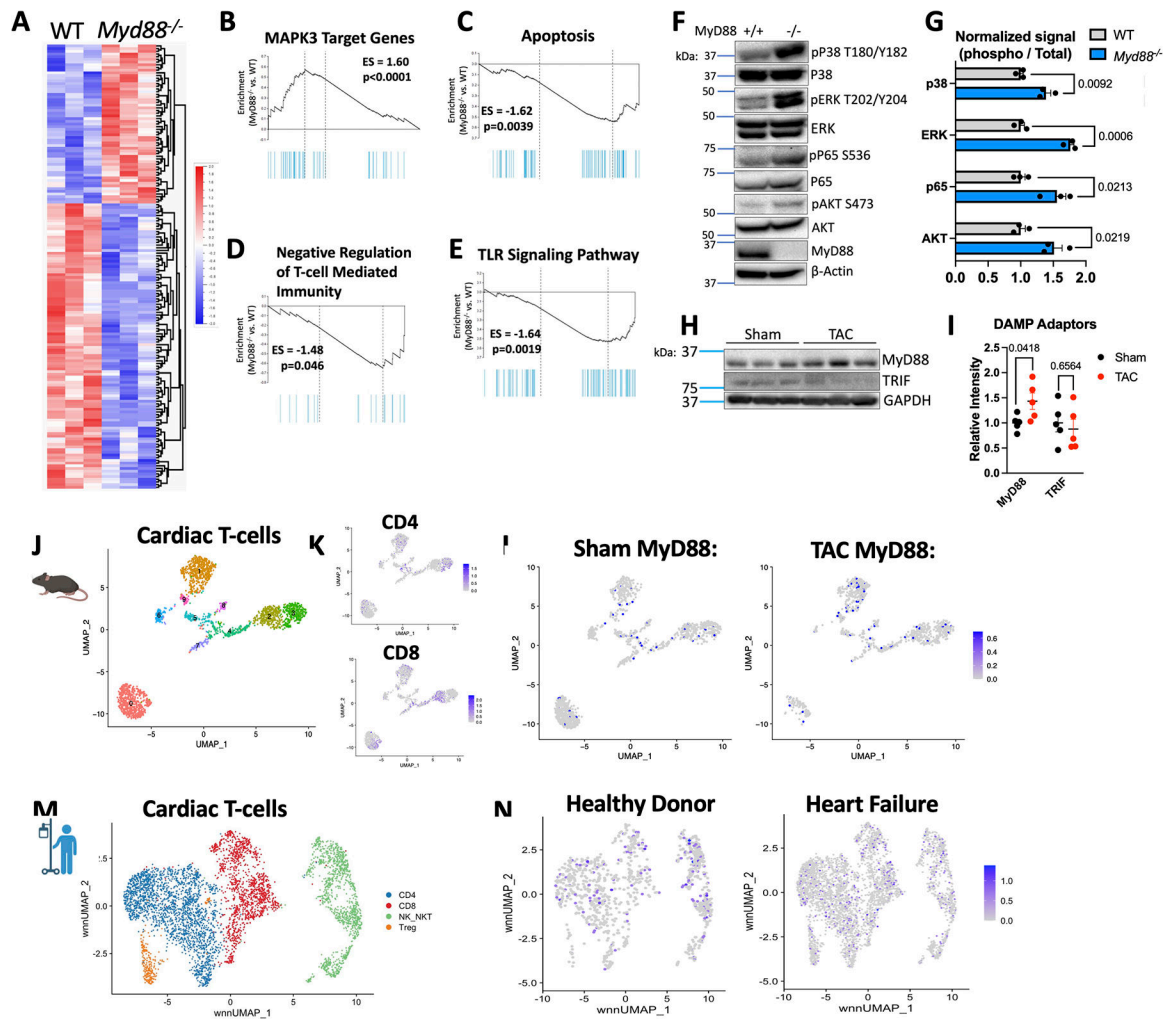


**Figure 2: MyD88 Regulates T-cell Signaling *In vitro* and In the Heart**

A. Bulk RNA sequencing was performed using RNA from  $n=3$  WT or *Myd88*<sup>-/-</sup> Th1 cells, shown are differentially expressed genes with hierarchical clustering using  $p < 0.05$  for significance. B-E. Selected gene set enrichment analysis from Bulk RNA-seq data, shown enriched in *Myd88*<sup>-/-</sup> Th1 cells as compared to WT. F. Representative western blot from WT or *Myd88*<sup>-/-</sup> Th1 cells, quantified in G. from  $n=3$  independent experiments and normalized to WT signal. H. Representative western blot from the LV WT mice after 4 weeks TAC or Sham surgery, quantified in I. for  $n=5$  mice total. J. Pooled 4 week Sham and TAC UMAP of total cardiac T-cells with overlay of *Cd4* or *Cd8a* expression (K). M. Relative *Myd88* expression in Sham vs. TAC T-cells clusters. N. UMAP of T-cells from pooled patient heart samples. O. Relative expression of *Myd88* in healthy donors or patients with heart failure. Statistical analyses by multiple T-tests (panels G-I), p values shown.

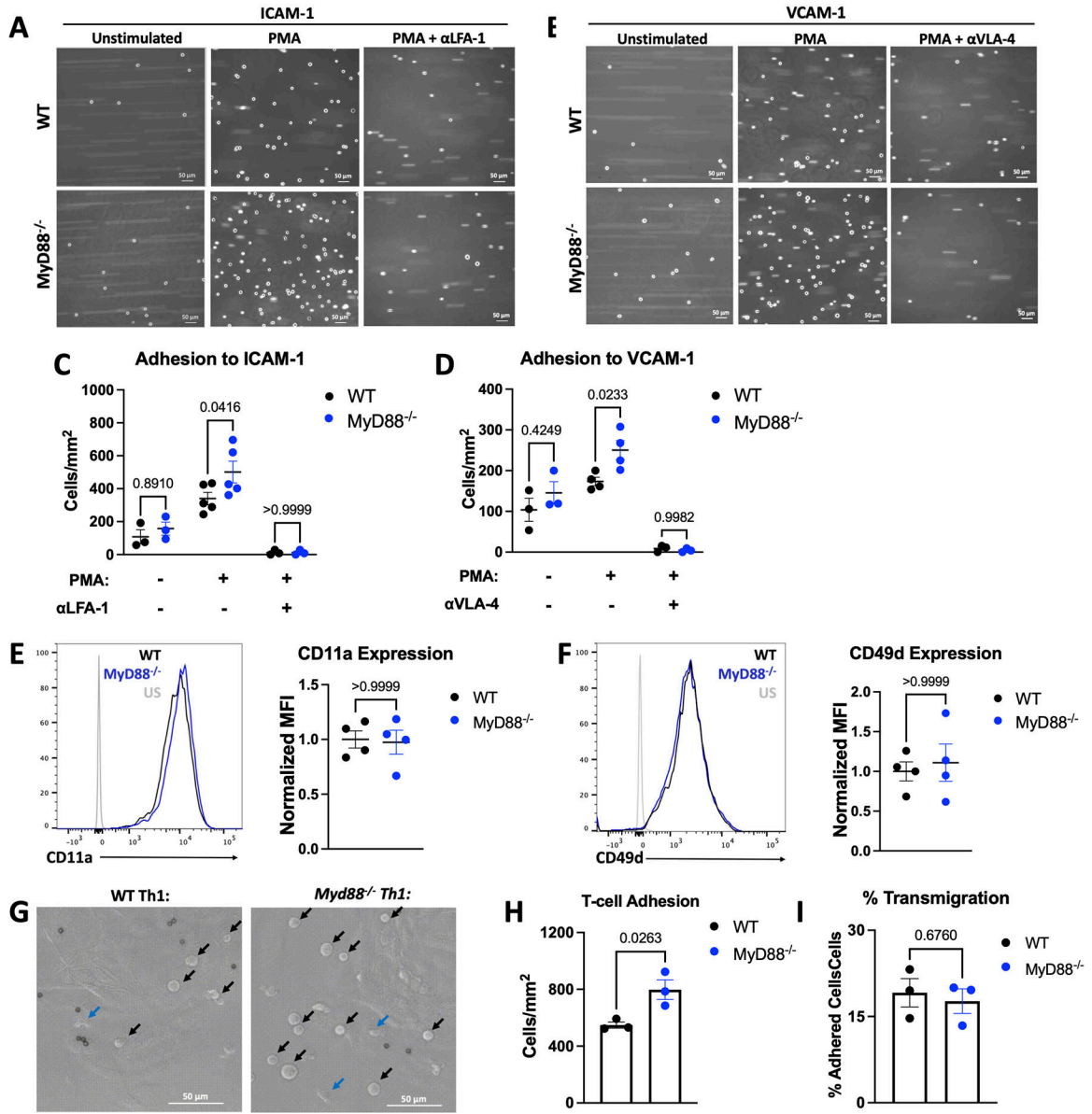


**Figure 3: MyD88 Deletion Increases Th1 Adhesion Ability Without Impairment of Transendothelial Migration**

A-D. WT or *Myd88*<sup>-/-</sup> Th1 cells were perfused at 1 million cells / mL at an estimated shear stress of 1 dyne / cm<sup>2</sup> over ICAM-1 or VCAM-1 after 5 minutes of treatment with 50 ng/mL PMA and/or 20 minutes of treatment with 20  $\mu$ g/mL  $\alpha$ LFA-1 or  $\alpha$ VLA-4 where indicated, shown are representative images (A-B), quantified in C-D. E-F. Representative flow cytometry plots from WT or *Myd88*<sup>-/-</sup> Th1 cells shown with quantification of n=4 independent experiments. G. 1 million WT or *Myd88*<sup>-/-</sup> Th1 cells were perfused over mouse heart endothelial cells pre-treated with 125 ng/mL TNF $\alpha$  for 4 hours, at an estimated shear stress of 1 dyne / cm<sup>2</sup>, at 37°C. TEM was monitored over 10 minutes and adhered vs. migrated cells were counted manually. Representative images of adhered cells (black arrows) vs. transmigrated cells (blue arrows) in G. with quantification of adhesion in H. and percent migration (migrated / adhered) in I. In all panels each data point is from an

independent experiment. All scale bars are 50  $\mu$ M. Statistical analysis by 2-way ANOVA with Sidák's multiple comparison test (C,D), Mann-Whitney Test (E, F) or T-test (H, I), p values shown.

Author Manuscript

Author Manuscript

Author Manuscript

Author Manuscript

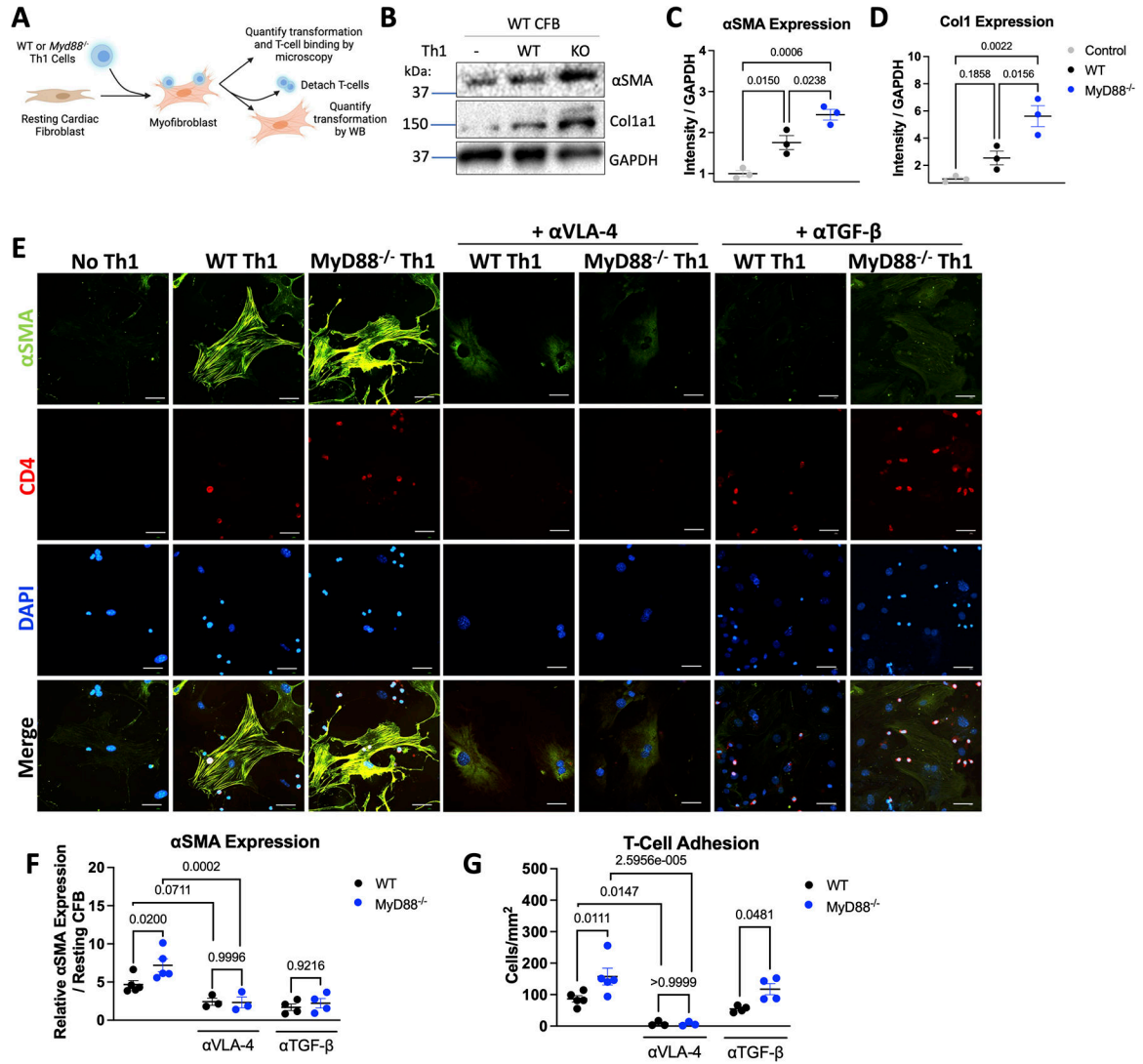


**Figure 4: *MyD88*<sup>-/-</sup> Th1 Cells Exhibit Increased Binding to and Activation of Fibroblasts**  
 A. Schematic of T-cell fibroblast co-cultures. WT cardiac fibroblasts were cultured with WT or *Myd88*<sup>-/-</sup> Th1 cells at a ratio of 2:1 CFB:Th1 for 16 hours with 20 μg/mL αVLA-4 or 5 μg/mL αTGFβ where indicated, non-adherent T-cells were washed off with PBS, and where indicated T-cells were detached with 5 mM EDTA. B. Representative western blot from cardiac fibroblasts after detaching WT or *Myd88*<sup>-/-</sup> Th1 cells, quantified using ImageJ for in C/D. E. Fibroblasts were stained for αSMA and CD4, and imaged by immunofluorescence microscopy. Representative images shown in E. αSMA was quantified using imageJ and normalized to untreated cells (F) and T-cells adhered were counted manually (G). Each data point represents an independent experiment. Scale bars are 50 μM. Statistical analysis by 1-way ANOVA with Tukey’s multiple comparison test (C-D) or 2-way ANOVA with Sidák’s multiple comparison test (F-G) with p values shown.

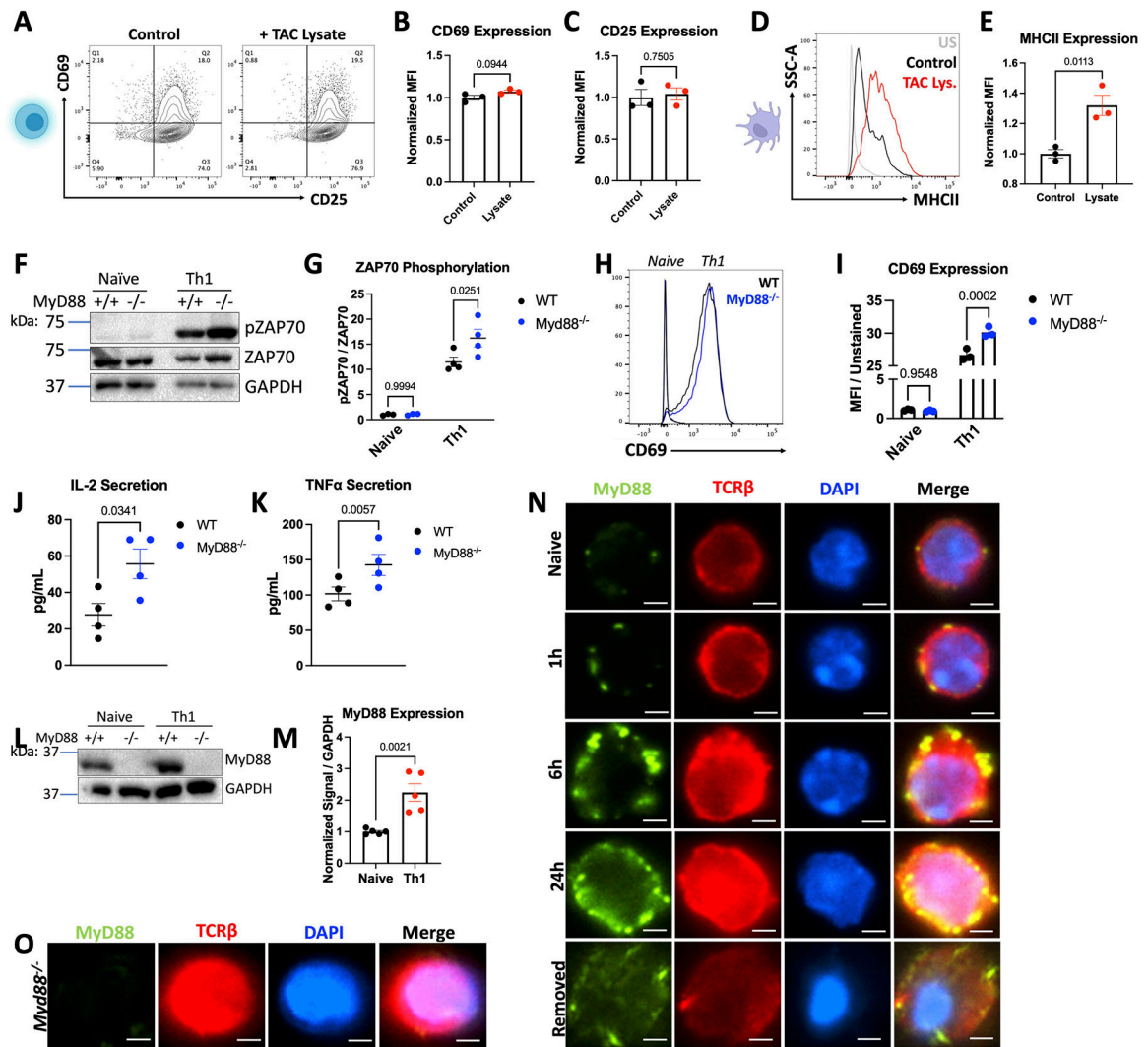


**Figure 5: MyD88 Acts as a Break During T-cell Activation through TCR but not TLR signaling**  
 Th1 cells were cultured in T-cell media with 10  $\mu\text{g}/\text{mL}$  of lysate generated from the LV of WT TAC mice for 24 hours, then analyzed by flow cytometry. Example plots shown in in A. with quantification for n=3 independent experiments in B-C. D-E. BMDCs were cultured with 10  $\mu\text{g}/\text{mL}$  of TAC lysate for 24 hours, then analyzed by flow cytometry. Representative plots shown in D, with quantification for n=3 independent experiments in E. F. Representative western blots from WT or *Myd88*<sup>-/-</sup> Th1 cells, quantified in G. WT or *Myd88*<sup>-/-</sup> Naive CD4<sup>+</sup> splenocytes or Th1 cells were stained and analyzed by flow cytometry, with representative plots shown in H. quantified in I. from n=3 independent experiments. J-K. Supernatants were collected for ELISA from 1 million WT or *Myd88*<sup>-/-</sup> Th1 cells cultured in fresh T-cell media for 24 hours from n=4 independent T-cell preps. L. Representative western blots from WT or *Myd88*<sup>-/-</sup> Naive CD4<sup>+</sup> or Th1 cells, quantified in M. from n=4 independent experiments. N-O. Naïve WT (N) or *Myd88*<sup>-/-</sup> (O) T-cells were plated on coverslips in the absence or presence of  $\alpha\text{CD3}/\text{CD28}$  for the indicated timepoints, or removed from stimulation for 24 hours, then stained with MyD88 and TCR $\beta$  for analysis



by fluorescent microscopy. Scale bars are 2  $\mu$ M. Statistical analysis by T-test (B,C, E, J, K, M), or 2-way ANOVA with Sidák's multiple comparison test (G, I) P values shown.

Author Manuscript

Author Manuscript

Author Manuscript

Author Manuscript

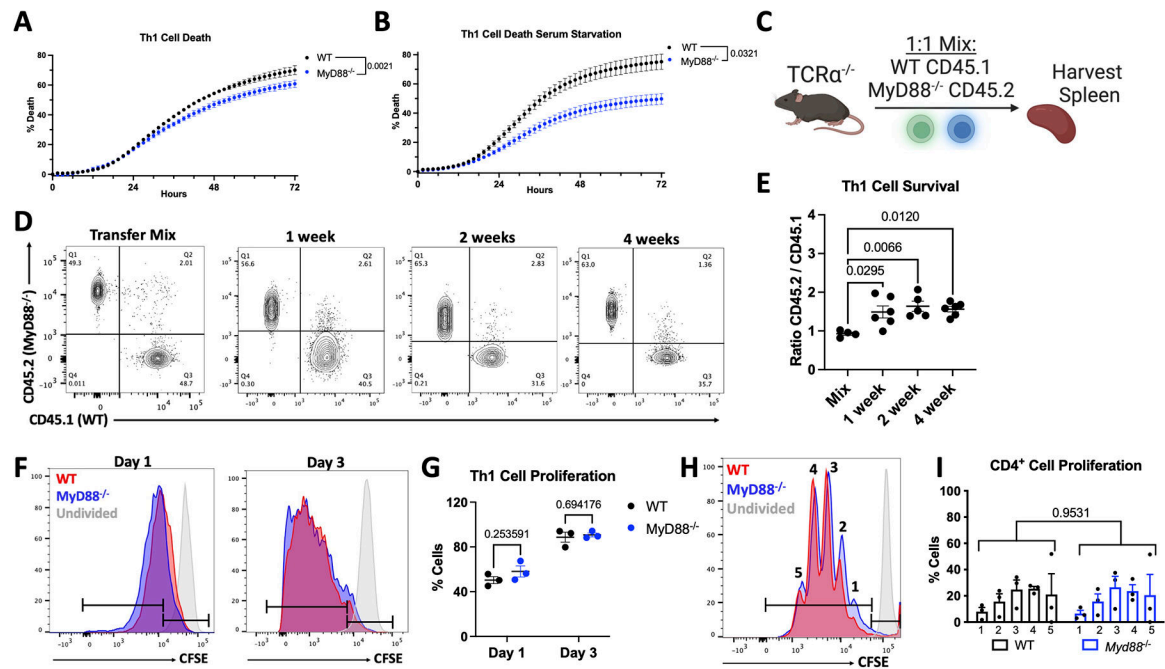


**Figure 6: MyD88 Knockout Enhances Survival but Not Proliferation in Th1 Cells**

A. WT or *Myd88*<sup>-/-</sup> Th1 cells were cultured on  $\alpha$ CD3 coated plates (10  $\mu$ g/mL) in the presence of 10  $\mu$ g/mL PI in media with or without 10% FBS. PI incorporation was monitored for 72 hours, baseline subtracted, and normalized to a 100% death Triton-X treated control. C. Scheme of *in vivo* competitive survival, in which healthy *Tcr $\alpha$* <sup>-/-</sup> mice were reconstituted with 10 million WT CD45.1 and *Myd88*<sup>-/-</sup> CD45.2 Th1 cells in 1:1 abundance, then spleens were harvested at indicated time points. D. Example flow cytometry plots gated on CD4<sup>+</sup>TCR $\beta$ <sup>+</sup> cells from *in vivo* survival showing transfer mix, then splenocytes after 1, 2, and 4 weeks, quantified in E. from 5–6 mice / group. F. Activated Th1 cells were stained with CFSE then cultured in the presence of 25U/mL IL-2 and collected after 1 or 3 days, example flow cytometry plots shown in F. quantified in G. from n=3 independent experiments. H. Naïve CD4<sup>+</sup> T-cells (CD62L<sup>hi</sup>CD44<sup>low</sup>) were sorted from splenocytes of WT or *Myd88*<sup>-/-</sup> mice, stained with 5  $\mu$ M CFSE, then polarized to Th1 cells as described in methods and collected after 3 days activation, representative plot in H. quantified in I. from n=3 independent experiments. Statistical analysis by 2-way ANOVA with repeated measures (A, B), 2-way ANOVA with Sidák's multiple comparison test (I), 1-way ANOVA with Tukey's multiple comparison test (E), or multiple T-tests (G), with n.s. = no significance, p values shown.

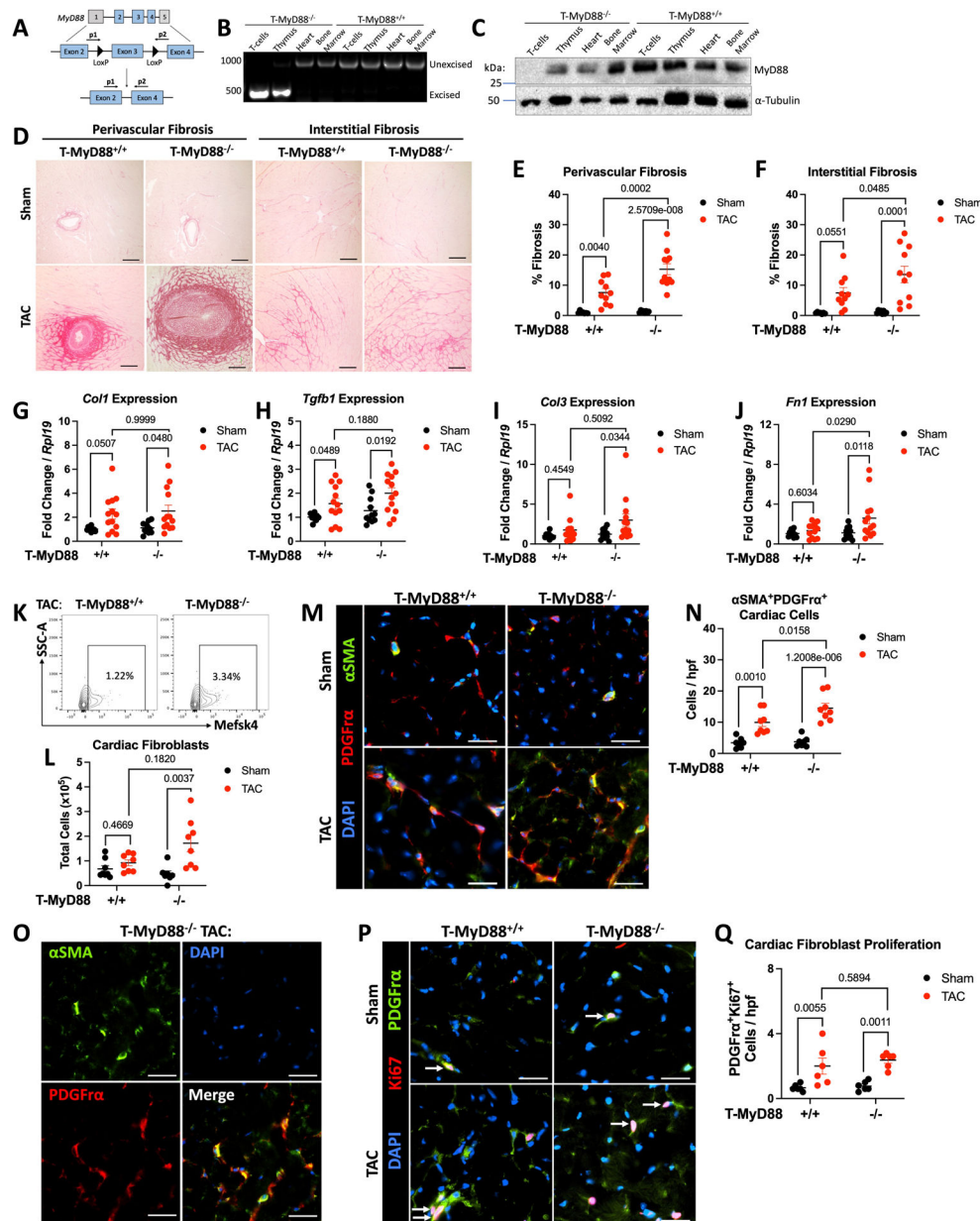


**Figure 7: T-Cell Specific MyD88 Knockout Mice Show Increased Cardiac Fibrosis with Increased Cardiac Fibroblast Activation and Proliferation**

A. Schematic showing *Myd88* floxed exon 3 and primers used to detect Cre-mediated excision. B. Genomic DNA was isolated from CD4<sup>+</sup> T-cells and control tissues and amplified to detect *Myd88* excision by PCR. C. Western blot of CD4<sup>+</sup> T-cells and control tissues for MyD88 deletion. D. 8–10 week male and female *Myd88<sup>fl/fl</sup>CD4<sup>Cre</sup>* mice using Cre<sup>+</sup> and Cre<sup>-</sup> littermates underwent 27G TAC or Sham surgery. Representative images from LV samples stained with Picrosirius, scale bars are 100  $\mu$ M. E-F. ImageJ was used to quantify fibrosis F in perivascular or interstitial regions respectively. G-J. RNA was isolated from the LV of each group of mice for gene expression analysis by RT-qPCR. K. The LV of each group of mice was enzymatically and mechanically digested for analysis of cardiac fibroblasts (CD45<sup>-</sup>Mefsk4<sup>+</sup>) by flow cytometry, shown are representative plots from TAC

mice (K) with quantification (L). M-N. Representative images from LV samples stained for  $\alpha$ SMA and PDGF $\alpha$ , scale bars are 25  $\mu$ M, with quantification in N. and individual channels shown in O. for a Cre+ TAC example. P-Q. Representative images from LV samples stained for PDGF $\alpha$  and Ki67, scale bars are 25  $\mu$ M, with quantification in Q. Each data point represents an individual mouse. Statistical analysis by 2-way ANOVA with Sidák's multiple comparison test (E,F,H,J,L), Kruskal-Wallis Test with Dunn's multiple comparisons test (G,I,N,Q), p values shown.

Author Manuscript

Author Manuscript

Author Manuscript

Author Manuscript

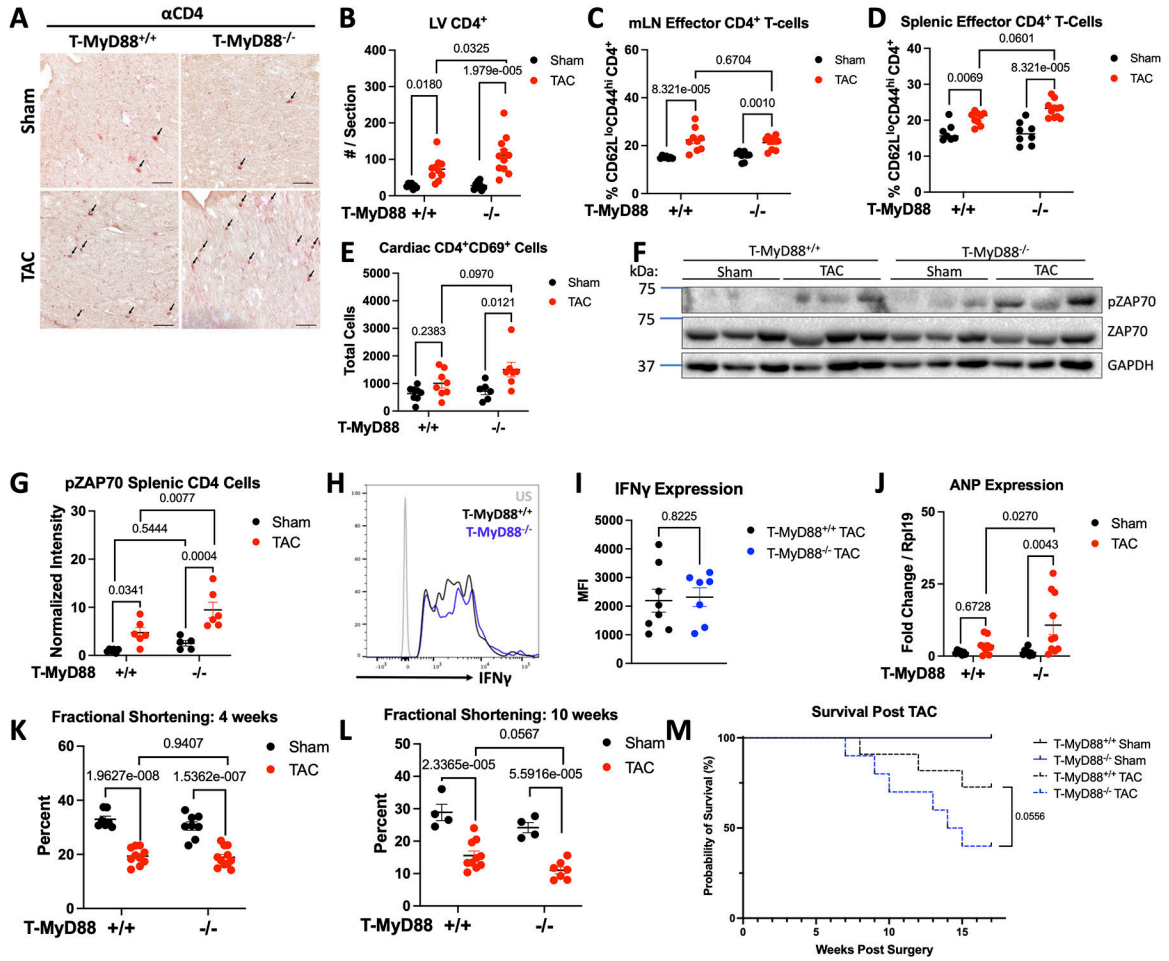


**Figure 8: T-Cell Specific MyD88 Knockout Mice Show Increased T-cell Activation, Cardiotropism, Systolic Decline, and Survival**

A. 8–10 week male and female *Myd88<sup>fl/fl</sup>CD4<sup>Cre</sup>* mice using Cre<sup>+</sup> and Cre<sup>-</sup> littermates underwent 27G TAC. Representative images from LV samples stained for CD4 with IHC, scale bars are 50  $\mu$ M, with quantification in B. C-D. The mediastinal lymph nodes and spleen of each group of mice was digested and effector T-cells (TCR $\beta$ <sup>+</sup>CD4<sup>+</sup>CD62L<sup>lo</sup>CD44<sup>hi</sup>) were quantified by flow cytometry. E. The LV of each group of mice was enzymatically and mechanically digested for analysis of cardiac T-cell reactivation (CD45<sup>+</sup>CD4<sup>+</sup>CD69<sup>+</sup>) by flow cytometry. F-G. Splenic CD4<sup>+</sup> cells were isolated from each group of mice for analysis of Zap70 phosphorylation, shown is a representative blot from 3 mice / group (F) with quantification of 6 mice (G). H-I. The mediastinal lymph nodes were digested and stimulated with PMA, Ionomycin, Brefeldin, and Monensin A for 4 hours before analysis of IFN $\gamma$  expression by flow cytometry, shown are representative plots (H) with quantification in I. J. RNA was isolated from the LV of each group of mice for gene expression analysis by RT-qPCR. K-L. Fractional shortening was measured by echocardiography at 4 weeks post surgery (K.) or 10 weeks post surgery (L). Each data point represents an individual mouse. M. Survival of *Myd88<sup>fl/fl</sup>CD4<sup>Cre</sup>* mice after 27G TAC analyzed by Mantel-Cox test. (n=4 Sham mice per each genotype, n=11 T-MyD88<sup>+/+</sup>

TAC, n=10 T-MyD88<sup>-/-</sup> TAC). Statistical analysis by 2-way ANOVA with Sidák's multiple comparison test (All except I) or T-test (I), p values shown.

Author Manuscript

Author Manuscript

Author Manuscript

Author Manuscript